Surface Charging Formulations for Engineering Applications. Validation by Experiments and Transient Models

Andreas Blaszczyk, Thomas Christen, Hans Kristian Meyer, and Michael Schueller

Abstract Electrostatic BEM (Boundary Element Method) formulations are presented for the calculation of dielectric surface charging, including saturation and restrike phenomena. The simulation results turn out to be in agreement with surface potential measurements in a simple rod-barrier-plane configuration, where lightning impulses initiate streamers and charge accumulation on the barrier. The usefulness of the given BEM-formulation is additionally supported by transient charging simulations in the framework of an electric carrier drift model.

1 Introduction

Surface charges (SC) on solid insulator surfaces can significantly influence the dielectric performance of medium and high voltage power devices. They can mitigate discharge inception effects during a lightning impulse test, as well as enhance them for applied voltages with reversed polarity. Unfortunately, the simulation of the intrinsically transient charging, which may occur via a zoo of different gas discharge processes like streamers, leaders, ion motion and combinations thereof, is a complex task and thus requires simplified approaches for application to real devices.

Recently a simplified engineering approach based on the saturation-charge boundary-condition has been proposed [1]. It works because saturation is a rather robust extremal stage of SC accumulation that allows assessment of possible changes in field

Andreas Blaszczyk, Thomas Christen
ABB Corporate Research 5405 Baden-Dättwil, Switzerland, e-mail: Andreas.Blaszczyk@ch.abb.com, Thomas.Christen@ch.abb.com

Hans Kristian Meyer
Norwegian University of Science and Technology (NTNU), Trondheim, Norway, e-mail: hans.meyer@ntnu.no

Michael Schueller
University of Applied Sciences Rapperswil, Switzerland, e-mail: michael.schueller@hsr.ch

distribution without performing the full analysis of the charging process. By neglecting the influence of the space charge, a simple electrostatic computation based on integral approach is possible (without meshing the gas volume).

In this paper we present a new formulation of the saturated SC for the 3D boundary element method (BEM), which can be efficiently applied in an industrial design environment. In addition to the saturation stage, computational models for modification of the accumulated charge due to restrikes (back discharges after changes of electrode potentials) are considered. The new formulation is validated with experiments and transient models.

2 BEM Formulations

The formulations presented below are explained and validated for a simple, air-insulated arrangement of rod-barrier-plane shown in Fig. 1 where the standardized lightning impulse (LI) 1.2/50 μs is applied to the active rod electrode. During the transient load and the dynamically developing discharge we distinguish a few representative stages shown in Fig. 1a-e. They occur within a time frame starting from 1 μs, when the applied voltage reaches the peak, up to 2-3 minutes lasting until the final measurement. Each of these stages can be represented by a steady state (electrostatic) formulation that is described in the following subsections. Such steady state formulations are applicable for arbitrary 3D geometries and can be efficiently used in engineering simulations [2].

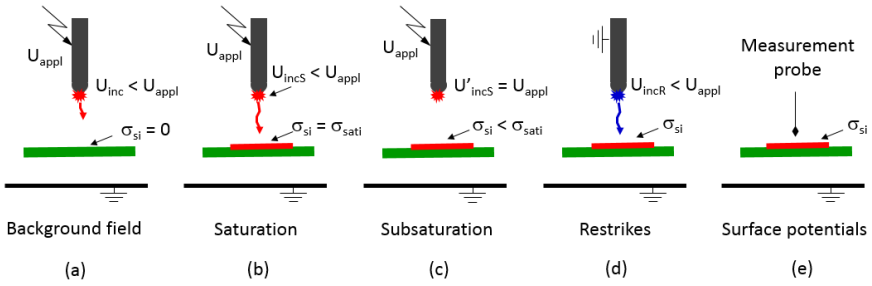

Fig. 1 Rod-barrier-plane configuration for different stages of discharge development.

The presented equations are limited to boundaries between gas and the solid dielectric where the surface charge distribution has to be obtained or specified. Other parts of the traditional BEM formulation including the Fredholm integral equation of the first order for electrode boundaries as well as formulation for floating potentials are described in [2] - [5].

2.1 Background Field

For a point i on a dielectric boundary the Gauss law must be fulfilled according to the following equation:

$$\varepsilon_{rIns}\varepsilon_0 E_{ni,Ins} = \varepsilon_{rGas}\varepsilon_0 E_{ni,Gas} + \sigma_{si} \tag{1}$$

where $\varepsilon_{r,Ins}$ and $\varepsilon_{r,Gas}$ are the relative permittivities of the solid insulation and gas, $E_{ni,Ins}$ and $E_{ni,Gas}$ are normal components of the electric field in the corresponding medium, and σ_{si} is the density of the accumulated surface charge, which is equal to zero in case of the initial background field, see Fig. 1a.

The indirect BEM formulation introduces a concept of virtual charge "in vacuo" that specifies the density σ_i for all points i on boundaries of the model as a solution of the equation system including (1) . Once this charge is obtained the field can be computed as a superposition of all virtual charge contributions. An essential feature is handling of the singularity when the field is computed exactly at the point i. This is solved by introducing a jump term resulting from the Gauss law applied to the virtual charge located on a small, flat surface area around the point i [4]. Consequently, the normal field components in (1) can be computed as a sum of a jump term and the normal electric field component E_{ni}^{-} obtained by integrating all virtual charges σ_j except of the charge located within the small, flat surface area around the point i :

$$E_{ni,Ins} = E_{ni}^{-} - \frac{\sigma_i}{2\varepsilon_0} \quad \text{and} \quad E_{ni,Gas} = E_{ni}^{-} + \frac{\sigma_i}{2\varepsilon_0} \tag{2}$$

with

$$E_{ni}^{-} = \frac{1}{4\pi\varepsilon_o}\sum_j \int_{S_j} \frac{\mathbf{n_i}\cdot\mathbf{r_{ij}}}{r_{ij}^3}\sigma_j dS \tag{3}$$

where $\mathbf{n_i}$ is the normal vector at collocation point i pointing into the gas and r_{ij} is the distance between collocation point i and the surface element represented by the integration point j [1]. After applying (2) to (1) and assuming $\sigma_{si} = 0$ one can obtain the Fredholm integral equation of the second order as follows:

$$E_{ni}^{-} - \frac{\varepsilon_{r,Ins} + \varepsilon_{r,Gas}}{\varepsilon_{r,Ins} - \varepsilon_{r,Gas}} \frac{\sigma_i}{2\varepsilon_0} = 0. \tag{4}$$

As shown in Fig. 1a, a streamer discharge will start to propagate if the applied voltage U_{appl} (peak value) is larger than the inception voltage U_{inc} at the rod tip (estimated according to [1]). This will deliver the charge to be accumulated along the barrier surface.

[1] Rigorous mathematical formulations denote the integral included in (3) as the adjoint double layer potential operator. Since our focus is on physical and engineering models the mathematical technique of computing this integral is beyond of scope of this paper. For more details we refer to literature [4], [5]

2.2 Saturation

We assume that the saturation stage at the dielectric boundary is achieved when the amount of accumulated charge is so large that the normal component of the electric field in the gas $E_{ni,Gas}$ is zero. Physically, it means that the accumulated charge changes the background field in such a way that the streamer discharge instead of hitting the barrier will follow the field lines going parallel to its surface, which will prevent further accumulation. Consequently, the equation (1) can be split into the following two equations where the prescribed surface charge density σ_{si} is replaced by the unknown saturation charge density σ_{sati}:

$$\varepsilon_{rGas}\varepsilon_0 E_{ni,Gas} = 0 \quad \text{and} \quad \varepsilon_{rIns}\varepsilon_0 E_{ni,Ins} = \sigma_{sati} \tag{5}$$

After applying (2) to (5) we get a system of integral equations where the unknowns are both charge densities, the virtual σ_i related to BEM and the physical σ_{sati} representing the accumulated charge:

$$E_{ni}^{-} + \frac{\sigma_i}{2\varepsilon_0} = 0 \quad \text{and} \quad E_{ni}^{-} - \frac{\sigma_i}{2\varepsilon_0} - \frac{\sigma_{sati}}{\varepsilon_0\varepsilon_{r,Ins}} = 0 \tag{6}$$

An example of the computed saturation charge distribution σ_{sati} has been shown in Fig. 2b (bell-shaped curve). The saturation charge will mitigate the field strength at the rod tip and increase the inception voltage from U_{inc} to U_{incS}. The saturation charge can be considered as a good approximation of the accumulated charge if $U_{incS} < U_{appl}$, see Fig 1b. Otherwise, the formulation presented in the next subsection should be followed.

2.3 Subsaturation

In case of $U_{incS} > U_{appl}$ the streamers delivering charge to the barrier may be extinguished. Consequently, the saturation may not be achieved and the extremal value of σ_{sati} (calculated from (6)) has to be reduced as follows:

$$\sigma_{si} = k_{si}\sigma_{sati} \cong k_{sConst}\sigma_{sati} \tag{7}$$

where the reduction factor k_{si} is approximated, for simplification, by a constant $k_{sConst} \leq 1$ (to be independent of location i). The value of k_{sConst} needs to be estimated iteratively so that the original inception voltage in saturation stage U_{incS} will decrease to a new value U'_{incS} where $U'_{incS} = U_{appl}$. U'_{incS} is the inception voltage calculated with the presence of the reduced surface charge (7), see Fig 1c. If in the saturated stage $U_{incS} < U_{appl}$ then $k_{sConst} = 1$ and no iterations are required.

The reduced charge (7) applied together with (2) to the continuity equation (1) leads to the following BEM formulation:

$$E_{ni}^{-} - \frac{\varepsilon_{r,Ins} + \varepsilon_{r,Gas}}{\varepsilon_{r,Ins} - \varepsilon_{r,Gas}} \frac{\sigma_i}{2\varepsilon_0} = \frac{\sigma_{si}}{\varepsilon_0(\varepsilon_{r,Ins} - \varepsilon_{r,Gas})}. \tag{8}$$

2.4 Restrikes

Restrikes, called also back discharges, may occur due to changes of the applied voltage. For example, the maximum voltage applied to the rod during the standard lightning impulse test 1.2/50 μs lasts approximately a few microseconds. The rod is grounded after a few hundreds microseconds, see Fig 1d. Due to the charge accumulated on the barrier a new inception may be initiated at the grounded rod tip. The new discharge will bring the charge of the opposite polarity to the dielectric, which will recombine with the previously accumulated charge reducing its total amount by a value of $Q_{removed}$. We assume that in the new equilibrium the normal field strength component at the dielectric will converge to a constant value E_{nConst} within a surface region affected by the charge removal. For a collocation point i within this region the charge density σ_{si} calculated in saturation or subsaturation stage will be reduced by an unknown value $\sigma_{\Delta i}$. With these assumptions the continuity equation can be split in two separate equations like in (5), but the additional terms related to E_{nConst} and $\sigma_{\Delta i}$ must be included as follows:

$$\varepsilon_{rGas}\varepsilon_0 E_{ni,Gas} = \varepsilon_{rGas}\varepsilon_0 E_{nConst} \tag{9}$$

$$\varepsilon_{rIns}\varepsilon_0 E_{ni,Ins} = \varepsilon_{rGas}\varepsilon_0 E_{nConst} + \sigma_{si} - \sigma_{\Delta i} \tag{10}$$

After introducing (2) and moving all unknowns to the left hand side the following BEM formulation can be obtained:

$$E_{ni}^{-} + \frac{\sigma_i}{2\varepsilon_0} - E_{nConst} = 0 \tag{11}$$

$$E_{ni}^{-} - \frac{\sigma_i}{2\varepsilon_0} + \frac{\sigma_{\Delta i}}{\varepsilon_0\varepsilon_{r,Ins}} - \frac{\varepsilon_{r,Gas}}{\varepsilon_{r,Ins}} E_{nConst} = \frac{\sigma_{si}}{\varepsilon_0\varepsilon_{r,Ins}} \tag{12}$$

The unknown value of E_{nConst} requires an additional equation specifying the amount of removed charge as a fraction of the total accumulated charge:

$$\sum_i \sigma_{\Delta i} S_i = Q_{removed} = (1 - k_{rConst}) Q_{total} \tag{13}$$

where $\sigma_{\Delta i}$ is the surface charge density removed in a point i, S_i is the surface area assigned to point i and Q_{total} is the total amount of surface charge $Q_{total} = \sum_i \sigma_{si} S_i$. The factor k_{rConst}, representing the fraction of the remaining charge, has a value in the range between 0 and 1, which has to be estimated iteratively using the similar criterion like in subsection 2.3: the inception voltage initiating the re-strike U_{incR} should be equal to U_{appl}. The whole restrike computation can be skipped if initially $U_{incR} > U_{appl}$. Examples of the computed charge density (volcano-shaped curve) and normal field distributions are shown in Fig. 2b.

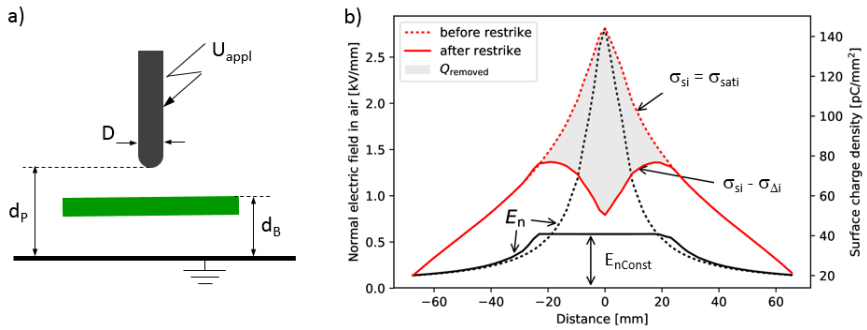

Fig. 2 (a) Rod-barrier-plane configuration. (b) distributions of charge density and normal field strength before and after the restrike calculated for: U_{appl}=35 kV, D=4 mm, d_P=10 mm, d_B=5 mm.

2.5 Surface Potentials

The last step in evaluation of surface charging is computation of the measured surface potentials. Typically a measurement has to be performed in a different geometrical configuration, which may significantly differ from the initial one used for background field, saturation and re-strikes. An example is shown in Fig. 1e where the active rod electrode has been replaced by a measurement probe (neglected in simulations). This requires re-computation of the whole model while preserving the already computed surface charge (The charge remains unchanged because in this stage all discharge activities are finished and no additional charge is delivered). For all charged points i the equations (7) and (8) can be used with the factor $k_{sConst} = 1$ or smaller if decaying effects should be considered.

3 Iterative Procedure

When using a static approach only snapshots of the final or intermediate charging stages can be evaluated. For complex geometrical configurations such an analysis is not straightforward and may require several computational steps in order to properly reflect the process of surface charge accumulation and the related discharge development. We propose an iterative procedure consisting of the following steps:

1. Compute electrostatic background field without any surface charge (4).
2. Find a location of saturation boundary condition and compute the corresponding saturation charge density according to (6):
   a. Evaluate the critical spots and identify points with the lowest inception voltage
   b. Select a discharge path starting from the most critical point and ending at a dielectric

c. Find and verify the surface patch for saturation boundary condition. This patch must fulfill the following criteria:
   - it must include the point where the discharge arrived (”seed point”)
   - the initial patch includes all neighboring points with the same orientation of the normal field component as in the ”seed point”
   - the polarity of the resulting charge density must be the same as the polarity of the discharge; points with the opposite polarity of surface charge density must be rejected
   - surface patches detached from the ”seed point” must be rejected
   - all points within the patch must fulfill the stability field criterion [1]: distance from the discharge start point is not larger than $U_{appl}/E_{stability}$.

   Note: For complex geometries the above procedure may require several steps (typically 2-4) including re-computation of saturation charge for the corrected patch. For simple examples like in Fig. 2 the surface patch represented by a circle of approximately 70 mm radius ($= 35kV/0.5kVmm^{-1}$) could be correctly defined within the first iteration.

3. Compute sub-saturation according to (7)-(8) if required.
4. Repeat steps 2 and 3 above if new inception points and possible discharges appeared due to computed surface charge. For example, the charge accumulated on the top of the barrier in Fig. 2a can trigger a new inception below the barrier, which will bring the charge of opposite polarity to the barrier bottom.
5. Compute re-strikes according to (11)-(13) if required.
6. Compute surface potentials for comparison with measurements.

4 Experimental Validation

The experimental test arrangement includes a HV rod with diameter D=7 mm (or 4 mm), a dielectric barrier 600x600x5 mm with $\varepsilon_{r,Ins}$=3, and a grounded plate electrode. The rod-barrier distance, d_B, and rod-plate distance, d_p, vary between 0 and 100 mm. A standard lightning voltage impulse (LI) with 1.2/50 μs and a peak value in the range between 20 and 100 kV is applied to the rod. The positive streamer discharge initiated at the spherical rod tip r=3.5 mm (or 2 mm) deposes SC at the barrier surface. After the impulse and a possible restrike the barrier together with the grounded plane are moved to another location where the surface potential due to accumulated charge is scanned by a robot-driven measurement probe. Before applying the next impulse the barrier is cleaned with alcohol in order to remove the SC.

For comparison between computations and experiments we selected 3 geometrical configurations representing different combinations of physical effects that have to be considered in the iterative procedure of section 3: **(a)** subsaturation with k_{sConst} = 0.975, Steps: 1,2,3,6; **(b)** re-strike with k_{rConst} = 0.95, Steps: 1,2,5,6; **(c)** charge accumulated on both barrier sides due to inception triggered by a small protrusion

placed at grounded plate under the rod, Steps: 1,2,4,6. The corresponding comparisons presented in Fig.3 show reasonable agreement. Multiple measurement curves illustrate the statistical behavior obtained when repeating the experiments. More experimental results are included in [6].

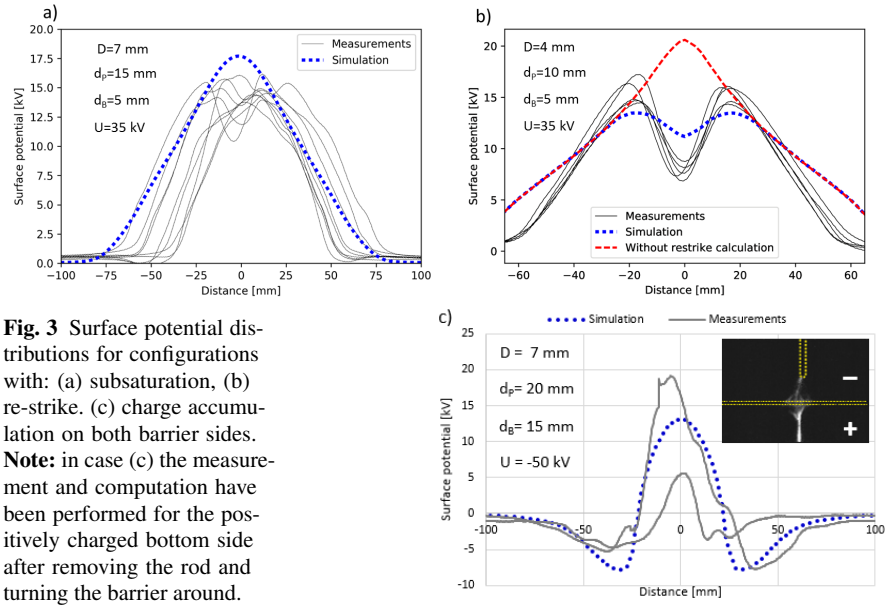

Fig. 3 Surface potential distributions for configurations with: (a) subsaturation, (b) re-strike. (c) charge accumulation on both barrier sides. **Note:** in case (c) the measurement and computation have been performed for the positively charged bottom side after removing the rod and turning the barrier around.

5 Validation with a Transient Drift-Diffusion Model

Surface charging is, in general, a dynamic process, and should thus be simulated with a transient simulation. Note that the iterative procedure discussed in Sect. 3 mimics a kind of transient charging. Of course, there are different types of charging processes, e.g., by streamers, Corona, or DC ion drift, etc. with different underlying physics and which may thus lead to different details of the final charge distributions. Here we show for a specific illustrative example that the previous approach, i.e., the nullification of the normal field component at the dielectric surface, reproduces well the result, which is obtained from a drift-diffusion model for space charge in a transient simulation. The details of the drift-diffusion model are described in Refs. [7,8] and will not be re-iterated here. It consists of the drift-diffusion equation for charge carriers with a mobility μ, which are injected from the contact. In principle, one can take into account in this model [7, 8] the effect of space charge in the Poisson equation, the effect of suppression of the inception in the electrode boundary condition model for charge injection, and the stability field in the carrier drift model. But

we will include here only the effect of the surface charge density, σ, in the Poisson equation, disregard all other effects, and compare the result with the assumption of normal field nullification used in Sect. 3. Surface charging is modeled by a local surface-charge source term on the solid dielectric surface, $d\sigma/dt = j$, where j is the normal component of the current density onto the dielectric surface. The surface charge density is thus just the time integral of the current density.

The cylindrically symmetric geometry allows to perform the simulations in 2d

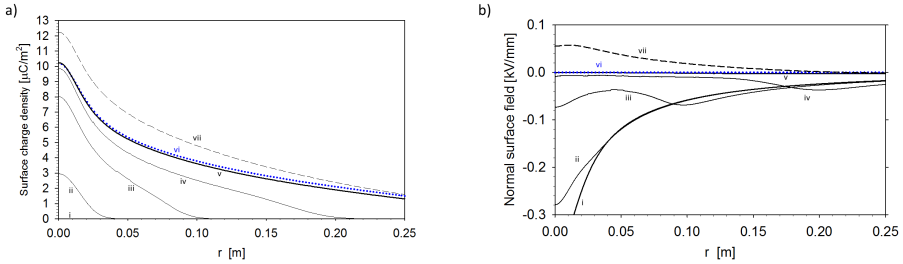

Fig. 4 a) Surface charge and b) normal surface field at different times during the transient charging up at 30 kV. i: capacitive state, ii: 0.2 μs, iii: 1 μs, iv: 10 μs, v: 100 μs, vi (blue dots): exact normal field nullification (Sect. 3), vii (dashed): with space charge (see text). c) Simulated final state: equipotential curves (blue), field lines (black), and surface charge (color) (the box contains a refined mesh).

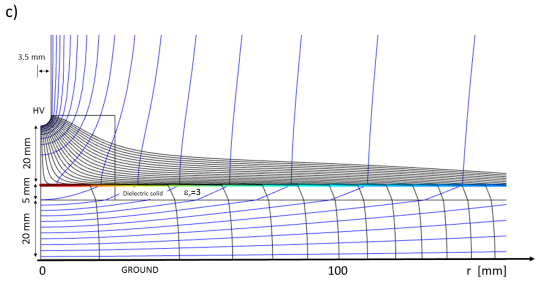

cylindrical coordinates (r,z); the geometrical details ($D = 7\ mm$, $d_p = 45\,mm$, $d_B = 25\,mm$) are sketched in Fig. 4. Furthermore, although we will not discuss details of the charging dynamics, we mention that there are two quantities which affect the duration of the charging process: the speed of the charge propagation, and the injection current density. The speed is generally very high for streamers as compared to, e.g., ion drift velocities. Although it is rather artificial to model streamers by a charge density cloud, we will assume a carrier mobility of $\mu \approx 1$ m^2/Vs, which leads in fields of the order of a few kilo-volts per millimeter to velocities which are comparable to typical streamer velocities. Nevertheless, due to the artificiality of the model, the mobility value should not be taken too serious but rather as a mean to control the characteristic time scale.

The simulation results are shown in Fig. 4. Parts a) and b) provide the space charge and field distributions, respectively, at different times during charging up. The final saturated state (curve v) is in good accordance with the normal field nullification approach obtained from a separate simulation, shown as curve vi. Of course, if one

includes further phenomena, like space charge effects, the normal field component does not necessarily vanish on charged surfaces. As an example, the dashed curves in Fig. 4a and 4b show the result for a case study, where the transient is simulated with taking space charge into account. The presence of space charge increases the accumulated saturation charge density by approximately 20 % (curve vii in Fig. 4a). After charging (steady state) the space charge is removed, such that the final field distribution is only due to the applied voltage and the surface charge. The normal field, which nullifies in presence of space charge, leads to a nonzero reversed field when the positive space charge is removed (curve vii in Fig. 4b). However, the inclusion of space charge can lead to a strongly nonlinear behavior (e.g., the formation of space charge limited currents [7, 8]), and requires additional justification and validation which is not the purpose here.

6 Conclusion

A comparison with experiments and transient modelling indicates that the numerically efficient steady-state surface charging model based on the discussed saturation concept can be used for a reasonable prediction of field characteristics during high voltage tests.

References

1. A. Blaszczyk, J. Ekeberg, S. Pancheshnyi, and M. Saxegaard. Virtual High Voltage Lab. SCEE 2016, Springer ser. Mathematics in Industry, Heidelberg 2018.
2. N. De Kock, M. Mendik, Z. Andjelic and A. Blaszczyk. Application of 3D boundary element method in the design of EHV GIS components. *IEEE Mag. on Electrical Insulation*, Vol.14, No. 3, pp. 1722, May/June 1998.
3. A. Blaszczyk, Region-oriented BEM formulation for numerical computations of electric fields SCEE 2008, Springer ser. Mathematics in Industry, Heidelberg 2010.
4. O. B. Tozoni, I. D. Mayergoyz: Calculation of three dimensional electromagnetic fields. Published by *Technika*, Kiev 1974 (in Russian language)
5. Z. Andjelic, B. Krstajic, S. Milojkovic, A. Blaszczyk, H. Steinbigler and M. Wohlmuth. Integral methods for the calculation of electric fields. *Scientific Series of the International Bureau Research Center Juelich*, 1992 (ISBN 3-89336-084-0).
6. H.K. Meyer, A. Blaszczyk, M. Schueller, F. Mauseth, A. Pedersen. Surface charging of dielectric barriers in short rod-plane air gaps - experiments and simulations. *IEEE Conf. on High Voltage Engineering and Application,* . ICHVE September 2018, Athens, Greece.
7. T. Christen. FEM Simulation of Space Charge, Interface and Surface Charge Formation in Insulating Media. *XVth International Symposium on High Voltage Engineering*, Ljubliana, Slovenia, 2007, 7, T8-54, 2007.
8. T. Christen. Nonstandard High-Voltage Electric Insulation Models. *Comsol Conference, Milano, Italy, (2012).*